# Human grasp point selection

**Urs Kleinholdermann**

Department of Psychology,
University of Giessen, Giessen, Germany

**Volker H. Franz**

Department of Psychology,
University of Giessen, Giessen, Germany
Department of Psychology,
University of Hamburg, Hamburg, Germany

**Karl R. Gegenfurtner**

Department of Psychology,
University of Giessen, Giessen, Germany

When we grasp an object, our visuomotor system has to solve an intricate problem: how to find the best out of an infinity of possible contact points of the fingers with the object? The contact point selection model (CoPS) we present here solves this problem and predicts human grasp point selection in precision grip grasping by combining a few basic rules that have been identified in human and robotic grasping. Usually, not all of the rules can be perfectly satisfied. Therefore, we assessed their relative importance by creating simple stimuli that put them into conflict with each other in pairs. Based on these conflict experiments we made model-based grasp point predictions for another experiment with a novel set of complexly shaped objects. The results show that our model predicts the human choice of grasp points very well, and that observers' preferences for their natural grasp angles is as important as physical stability constraints. Incorporating a human grasp point selection model like the one presented here could markedly improve current approaches to cortically guided arm and hand prostheses by making movements more natural while also allowing for a more efficient use of the available information.

## Introduction

### Grasping: Combining the basic rules

Many properties of the human grasp movement have been thoroughly studied. Much is known about the coupling between visual input and the grasp movement (Goodale, Pelisson, & Prablanc, 1986; Goodale, Milner, Jakobson, & Carey, 1991; Goodale et al., 1994; Whitney, Westwood, & Goodale, 2003), the processing of object features (Ganel & Goodale, 2003), and the cortical control of grasping (Cattaneo et al., 2005). Models for generating arm movement trajectories (Harris & Wolpert, 1998; Smeets & Brenner, 1999) are available. However, it is not possible to model the complete human grasp movement because what determines the choice of contact points with an object remains unclear. This is surprising, considering that important properties of the grasp movement like the grip aperture and its maximum are very well studied (Jeannerod, 1984, 1986; Smeets & Brenner, 1999) and seem to arise secondarily from the choice of appropriate contact points (Cuijpers, Smeets, & Brenner, 2004). Building upon previous work on human and robotic grasping, we identified the most important rules for choosing those points and combined them into a quantitative model of human grasp point selection for precision grip grasping.

The most important physical constraint in grasping is finding a grasp configuration that fulfills force closure. For two-digit grasping, this is the case when the grasp axis, a line connecting the two contact points, lies within the friction cones resulting from the friction coefficient between object and digits (Iberall, Bingham, & Arbib, 1986; Nguyen, 1986; Blake, 1992; Chen & Burdick, 1993). Force closure is a necessity for grasping and therefore is widely used in constructing stable grasps for robotic grippers (Blake, 1992, 1995; Ponce, Stam, & Faverjon, 1993). Grasping at points that do not satisfy force closure will lead to slippage of the object through the digits. In CoPS, force closure is represented by the parameter $\gamma$ (the sum of the angular deviances of the grasp axis from both friction cone center axes). The smaller $\gamma$, the better force closure is fulfilled. Force closure is optimal if points on the

object's surface are chosen that align the grasp axis with the central axes of both friction cones. In this case, $\gamma$ is zero.

The second constraint we identified is minimizing torque, which is related to the distance between the grasp axis and the barycenter of the object. Minimizing torque allows holding the object without much effort. This rule has been proposed and assessed earlier (Lederman & Wing, 2003; Lukos, Ansuini, & Santello, 2007) and has been used as a measure of grasp quality (Goodale et al., 1994). It is also included in models on synthesizing stable grasps for robot grippers (Mangialardi, Mantriota, & Trentadue, 1996; Sanz, Iñesta, & del Pobil, 1999). In CoPS, deviances from this rule are measured by the parameter $\tau$ (the product of object mass and torsion arm length, which is proportional to torque). When the torque rule is perfectly satisfied, $\tau$ is zero and the grasp axis passes through the barycenter.

Force closure is a physical necessity for grasping. Keeping the torque small is partly a physical constraint but also partly due to the physiological properties of a human grasper. Applying an extra amount of force, which could counteract a high torque, might be uncomfortable or even impossible. In contrast, our third constraint, the natural grasp angle (NGA), completely depends on the individual human grasper. The term natural grasp axis was coined for the finding that, for grasping a disc, a certain orientation of the grasp axis is preferred over all others (Lederman & Wing, 2003), although all grasp axes through the center of the disc are otherwise equally qualified for grasping. The NGA, being the angle of this axis, reflects the comfort of the grip for the grasper. This becomes obvious when trying to grasp an object with the positions of thumb and index finger reversed. The grasping arm then is contorted in an uncomfortable fashion. In the CoPS model we assume that people aim to use their personal NGA, which is constant for a certain location in egocentric space. Therefore, the NGA rule is perfectly satisfied when the difference $\alpha$ between the NGA and the actually realized grasp angle is zero.

Having identified the most important rules involved in grasp point selection, the question arises as to how they are combined to guide the digits to the most appropriate points. Deviations from any rule cause grasp failure or discomfort, which can be associated with a penalty in the motor system. Let $g$ be a grasp (i.e., an ordered pair of contact points of thumb and index finger). Every $g$ is then associated with a certain violation of the force closure rule $\gamma(g)$, the torque rule $\tau(g)$, and of the NGA rule $\alpha(g)$. The preference for certain values of $\alpha(g)$, $\tau(g)$, and $\gamma(g)$ can be modeled with a set of penalty functions $f_\alpha(\alpha)$, $f_\tau(\tau)$, and $f_\gamma(\gamma)$. A simple penalty function, which can cover a wide variety of different shapes while having only very few free

parameters, would be of the general form $f(x) = ax^b$. Here $a$ is a parameter responsible for the weighting of the rule and $b$ defines how quickly penalty values increase when rule deviation increases. Generally the function is symmetrical around 0, such that rule deviations are punished equally in both directions. The most simple way to combine the individual rule penalties so that each rule makes an independent contribution to the final penalty value for a particular grasp p($g$) is to sum them up:

$$p(g) = f_\alpha\big(\alpha(g)\big) + f_\tau\big(\tau(g)\big) + f_\gamma\big(\gamma(g)\big) \qquad (1)$$

The grasp associated with the lowest penalty value is then chosen for grasping.

Experiments 1 and 2 were conducted to estimate the model parameters $a$ and $b$ associated with each grasp rule. They were designed as rule-conflict experiments. Participants were forced to reveal to what extent they prefer to satisfy one rule at the cost of the other. Experiment 3 served as a validation of the model.

## Methods

### Participants

In Experiments 1, 2, and 3 we measured 17, 19, and 18 right-handed participants with three, five, and five of them being male, respectively. The mean age was 24 years in all three experiments (*SD*: 3, 4, and 3 years). Informed consent was obtained according to the Declaration of Helsinki. Methods and procedures followed the guidelines of the APA (American Psychological Association). Participants were paid eight euro (approx. $10.42) per hour.

### Stimuli

The stimuli of all three experiments were made of black plastic material (polyoxymethylene) with a density of 1.38g/cm$^3$. In Experiment 1 we used a disc of 2.5 cm radius and nine square blocks of 5 cm edge length. All objects had a height of 1.5 cm. In Experiment 2 we used a disc of 2.5 cm radius and nine ellipsoids with an extent of 10 cm along the major and 5 cm along the minor axis. Embedded in each ellipsoid was a clearly visible lead cylinder of 1.5 cm radius and 0.8 cm height, which was varied between objects along the major axis of the ellipse such that the barycenter moved from $-2$ to $+2$ cm in steps of 0.5 cm relative to the ellipse center. The weight of the ellipses was 89 g. All objects of this experiment and Experiment 3 had a height of 1 cm. Stimuli of Experiment 3 were one disc
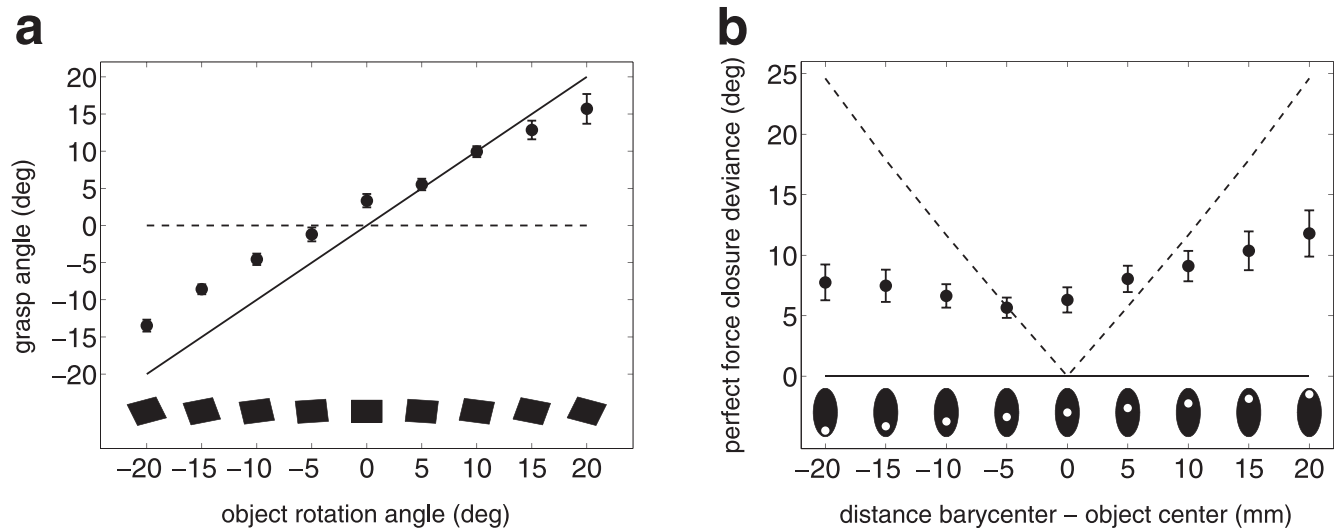
Figure 1. Results of grasp rule conflict in Experiments 1 and 2, along with the fitted penalty functions. (a) Mean realized grasp angle to the rectangular stimuli of Experiment 1. The solid line indicates grasp angles expected for perfect force closure. The dashed line denotes the grasp angle expected for no deviance from NGA. Rectangles in the bottom row schematically show the rotation of the stimuli used. (b) Mean realized angular deviance from perfect force closure ($\gamma$) in Experiment 2. The solid line indicates perfect force closure, which can be achieved by grasping the ellipse at its minor axis. The dashed line denotes the deviance values from perfect force closure associated with grasping the object at its shifted barycenter. Ellipses in the bottom row schematically show the position of the barycenter in the object. The intercept greater zero for the zero barycenter-object center distance object results because the force closure deviance is always positive and because of a general undershoot in participant's movements. On both panels, error bars depict +/-1 SEM between participants.

of 2.5 cm radius and nine objects of complex shape. The contours of these objects are pictured in Figure 5b. Their weight ranged between 38 and 56 g.

## Setup

Each participant was seated in front of a table with his or her head resting on a chinrest. The pod holding the stimuli was mounted at a distance of 36 cm from the chinrest in the participant's saggital plane. It could be rotated for adjusting the stimulus orientation to the individual NGA. At the right side of the participant, the movement's starting point, which consisted of a small plastic knob, was mounted at a distance of 36 cm from the object pod. Participants wore liquid crystal shutter glasses (Milgram 1987), which enabled us to obscure vision of the stimuli and the setup arrangement between trials. Movement recordings were done with an Optotrak 3020 (Northern Digital Inc., Waterloo, Ontario, Canada) infrared tracking system using a frequency of 200 Hz. Three infrared markers of the system were attached to the participant's index finger, and three infrared markers of the system were attached to the participant's thumb, respectively. The contact point on the fingertip of each digit was calibrated for every participant in relation to the three markers. In the experiments the contact points with the object then

were measured at the moment of object liftoff. To this end, we determined for both digits the moment in time where they reached their maximum acceleration in a direction orthogonal to the table surface after leaving the point of closest proximity with this surface. The value of the earlier digit was chosen as the moment of lift. These calculations were done on second order Butterworth filtered data with a cut-off frequency of 15 Hz.

## Procedure

In all experiments, participants were instructed to grasp the target object with a precision grip of index finger and thumb, lift the object, and carry it towards the experimenter who sat at their right side. The shutter glasses remained open for three seconds from trial onset and participants completed the whole movement during this time interval. Then the shutter glasses turned opaque and remained so until the start of the next trial.

Before each experiment, we used 6 to 10 practice trials, which were not included into the analysis. After this practice, 25 to 30 trials with a disc followed in order to determine the individual NGA. In Experiments 1 and 2 the experimenter then rotated the object holder according to the participant's NGA measured as
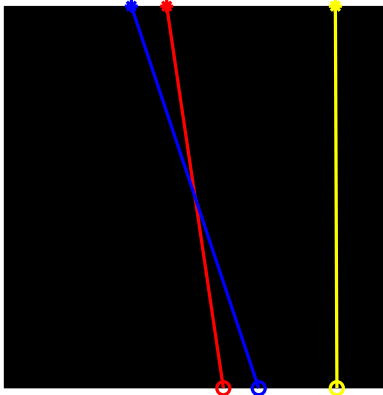
Figure 2. Equipenalty deviations from the force closure (red), the natural grasp angle (blue), and the torque rule (yellow). The figure shows three exemplary two-digit grasps (circle: contact point of the thumb, star: contact point of the finger) on a 50 g, 5 × 5 cm rectangular object. The natural grasp angle is defined to be the perfect vertical. From the equations of the CoPS model, the amount of penalty related to force closure deviation in the red set of contact points equals the amount of natural grasp angle deviation related penalty in the blue set and the amount of torque deviation related penalty in the yellow set. Note that the red and blue set of contact points show deviations on both the force closure and natural grasp angle rule, such that their overall penalty value according to the CoPS model differs from each other and from the overall penalty value for the yellow set of contact points.

the average grasp angle in the disc trials. The shutter glasses were opaque during the rotation and participants were told that the setup would be adjusted, without being given specifics about the adjustment. Then the experiment proceeded with the experimental trials using a random sequence of the stimuli described above. The random presentation was used in order to avoid an adaption to a particular stimulus and thus, arrive at more generalizable estimates for the penalty functions. Every stimulus was grasped ten times per participant.

### Experiment 1: Force closure versus grip comfort

Using the participant's NGA measured in the disc trials, one rectangular block (the neutral object) was aligned with one of its cardinal axes such that it could be grasped with zero deviance from perfect force closure, zero barycenter distance and zero deviance from the NGA ($\gamma = 0$, $\tau = 0$, $\alpha = 0$). Additionally, we used eight blocks rotated away from the participant's NGA, such that participants had to decide whether to follow the rotation with their digits. Following the rotation would ensure good force closure but would increase the deviation from the NGA. Distance to the block's barycenter (corresponding to the value of $\tau$) could always freely be chosen and thus did not

influence the values of the other two rules in this experiment.

### Experiment 2: Force closure versus grasp axis torque

Participants grasped ellipsoid shaped objects. All of them were aligned with their minor axis to the individual participant's NGA. One ellipsoid had its barycenter at the intersection of the major and minor axis (neutral object). It was possible to grasp it with zero deviance from perfect force closure, zero barycenter distance, and zero deviance from the NGA (neutral object, $\gamma = 0$, $\tau = 0$, $\alpha = 0$). For the remaining eight ellipsoids, the barycenter was shifted along the major axis. Participants had to choose whether to follow this shift with their grasp. Doing so would ensure a small distance to the barycenter and thus a small value of $\tau$. Due to the curved ellipse contour, however, it would result in a larger deviance from perfect force closure and thus enlarge $\gamma$. Because of the objects' alignment to the NGA the value of $\alpha$ did not influence the values related to the other two rules in this experiment.

### Experiment 3: Experimental validation

In Experiment 3 we used the same setup and procedure as in Experiments 1 and 2. We presented a new set of nine complex shaped objects (see Figure 5b for the contours) to our participants and a circular disc. Data from this experiment were used for testing the model predictions we could make using the results of Experiments 1 and 2 (see Data analysis section). We thus were able to do a validation of the model on a new dataset that hadn't been used in the process of estimating the free model parameters.

## Data analysis

From the data of Experiment 1 we estimated the penalty function for $f_\alpha$ relative to $f_\gamma$. We used $f_\gamma$ as reference function and thus set its weight to 1 and its power to 2, the lowest power, which would be used in a Taylor expansion to approximate a function symmetrically increasing around $x = 0$. As the value of $\tau$ could be chosen independently from $\gamma$ and $\alpha$ in this experiment, the penalty function for Experiment 1 reads

$$p(\alpha, \gamma) = f_\alpha(\alpha) + f_\gamma(\gamma). \qquad (2)$$

As the value of $\gamma$ was completely dependent on the chosen value of $\alpha$ and the object's angle of rotation $r$ (Equation 2) can also be expressed as

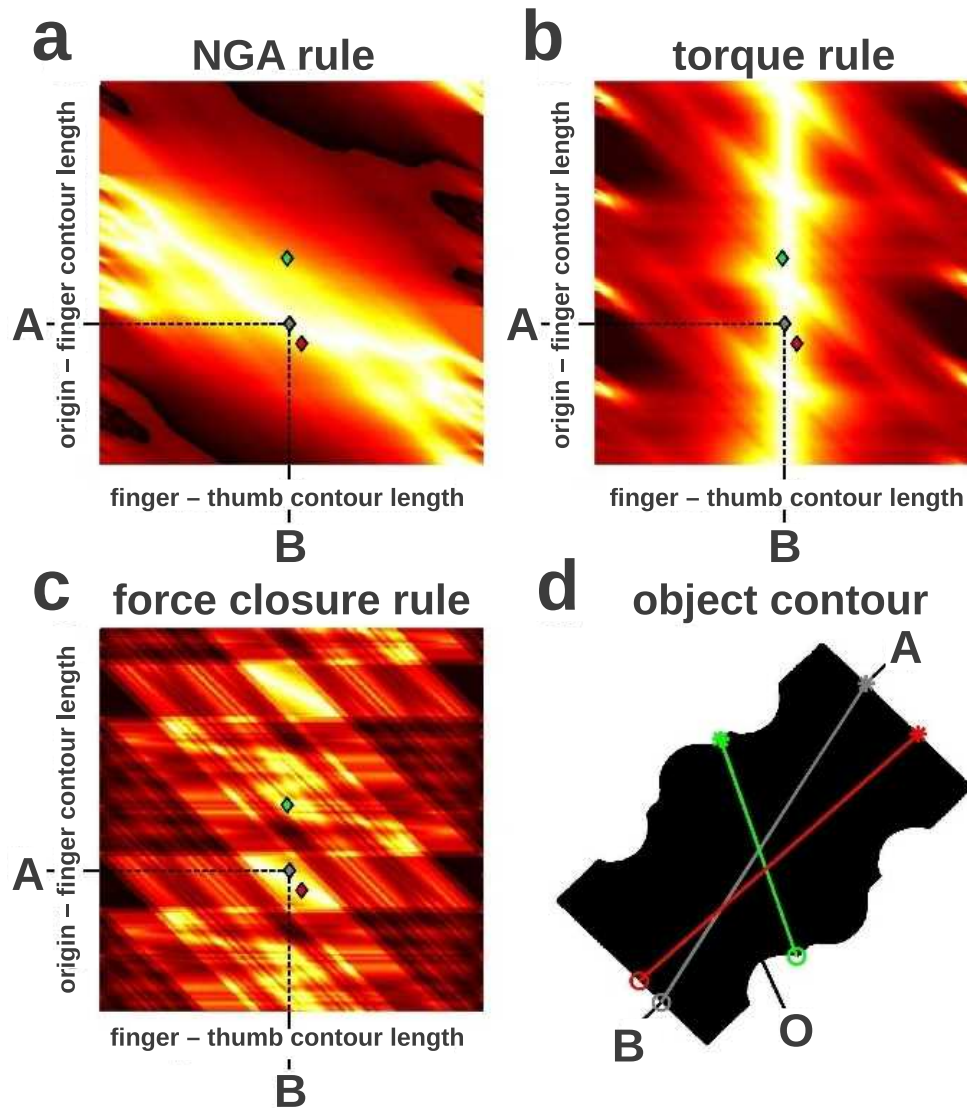$$p(\alpha, r) = f_\alpha(\alpha) + f_\gamma(\alpha, r). \qquad (3)$$

Figure 3. Example penalty maps for one of the objects used in Experiment 3. (a) natural grasp angle rule, (b) torque rule, (c) force closure rule, and (d) contour of the corresponding object. The CoPS model combines the individual penalty maps to a complete penalty map, as shown in Figures 4 and 5. In (a) through (c), the *y*-axis depicts the length from the position of the index finger along the contour of the object to the origin indicated in (d) as O, and the *x*-axis depicts the contour length between index finger and thumb, both measured counterclockwise. Consequently, every point in (a) through (c) corresponds to one grasp. The colors of the heat maps denote the penalty value of each grasp from low to high (low = white, yellow, red, black = high; for clarity, color values are adapted to the penalty range of each map). As an example, consider a participant grasping at point A with the index finger and at point B with the thumb. This grasp is depicted in (a) through (c) by a gray diamond. The grasp is favored by the CoPS model, because it shows zero deviation from the natural grasp angle, with white color in (a); zero distance to the barycenter, shown by white color in (b); and relatively small deviation from optimal force closure, shown by yellow color in (c). Two more exemplary grasps are shown in red and green, with circles and stars in (d) denoting thumb and index finger, respectively.

We estimated the coefficients $a$, $b$ of the penalty function

$$\mathrm{f}_\alpha(\alpha) = a\alpha^b \qquad (4)$$

by numerically minimizing the criterion value $c$ of the objective function

$$c = \sum_r \left( \frac{\delta}{\delta\alpha} \mathrm{p}(\alpha_r, r) \right)^2. \qquad (5)$$

The value of $\alpha$ depends on the configuration of the digits relative to each other but also on the rotation of the wrist. As the ease of a rotation in the wrist likely depends on rotation direction, we estimated separate
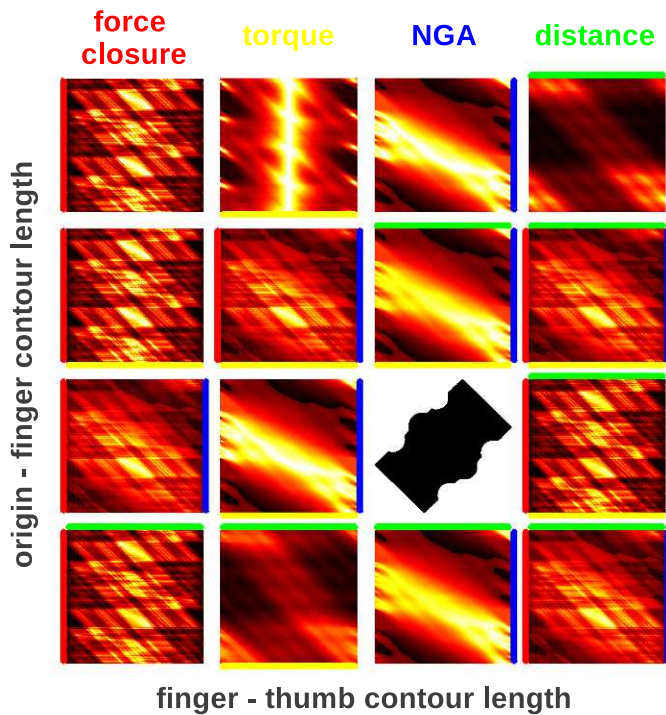
Figure 4. Penalty maps showing all possible combinations of penalty rules for the object of Figure 3. Every single map is created from one or more of the four grasp rules, as indicated by the color coded map borders. The top row shows maps for one rule only. The lower left triangle shows maps for two rules. For example, the lowest and leftmost map (row 4, column 1) is for the rules force closure (red) and distance (green). The remaining right upper triangle is filled with maps for all combinations of three rules (row 2, columns 2 and 3; column 4, rows 3 and 4) and, finally, the penalty map of the complete CoPS model containing all four rules is the rightmost element of the second row.

penalty functions for the objects rotated clockwise and counterclockwise away from the NGA respectively.

In Experiment 2 the value of $\gamma$ depended on the chosen distance $d$ of the intersection point of the grasp axis with the major ellipse axis to the ellipse center. The value of $\tau$ was dependent on the distance between this intersection point and the barycenter of the ellipse. Thus, $\tau$ could also be written as a function of $d$ and the position $k$ of the barycenter on the major ellipse axis. As the influence of $\alpha$ was negligible in this experiment, the penalty function thus could be expressed as

$$p(d, k) = f_\gamma(d) + f_\tau(d, k) \tag{6}$$

Inspecting the data of Experiment 2, we saw that participants' choice of contact points was biased towards shorter movement distances (see Results). Therefore we also included a penalty term for distance ($\lambda$). For the average rotation of the ellipse, $\lambda$ could also

be expressed as a function of $d$ thus Equation 6 was extended to

$$p(d, k) = f_\gamma(d) + f_\tau(d, k) + f_\lambda(d). \tag{7}$$

From the data of Experiment 2 we estimated for the torque rule the values of coefficients $a$ and $b$ of the penalty function

$$f_\tau(\tau) = a\tau^b. \tag{8}$$

For the distance rule, however, as distance had not been subject to a stepwise conflict with another rule, the observable average undershoot just allowed for the estimation of one coefficient

$$f_\lambda(\lambda) = a\lambda. \tag{9}$$

In order to estimate the coefficients we minimized the objective function

$$c = \sum_k \left( \frac{\delta}{\delta d} p(d_k, k) \right)^2. \tag{10}$$

Estimation of the coefficients was done using MATLAB R2007b with the Optimization Toolbox (The Mathworks, Inc., Natick, MA). Statistical testing was done using R version 2.14.1 (R Development Core Team, 2011). Shapiro–Wilk tests with a significance level of $\alpha = .05$ were used to test if differences are normally distributed. As this was not always the case, we used Wilcoxon's signed-rank test for the evaluation of the CoPS model using a quality index (see below).

## Simulation-based validation

In a second validation step, we wanted to test if the CoPS model makes a specific prediction for a particular object rather than a general guess valid for all objects presented in Experiment 3. We tested for this by changing the assignment between stimulus object and penalty values. This amounts to switching the penalty "map" of one object as shown in Figure 5 with that of another object.

## Analysis of individual grasp rules

In order to reassess the relative importance of the four grasp rules from the data of Experiment 3 we created five comparison models. Four of these models were lacking one of the rules present in the complete CoPS model. In the fifth comparison we used a modified model in which the penalty function for deviating from the NGA had been fitted onto both directions of deviation. Thus, the corresponding penalty value was the same regardless if the deviation was clockwise or counterclockwise. For all these
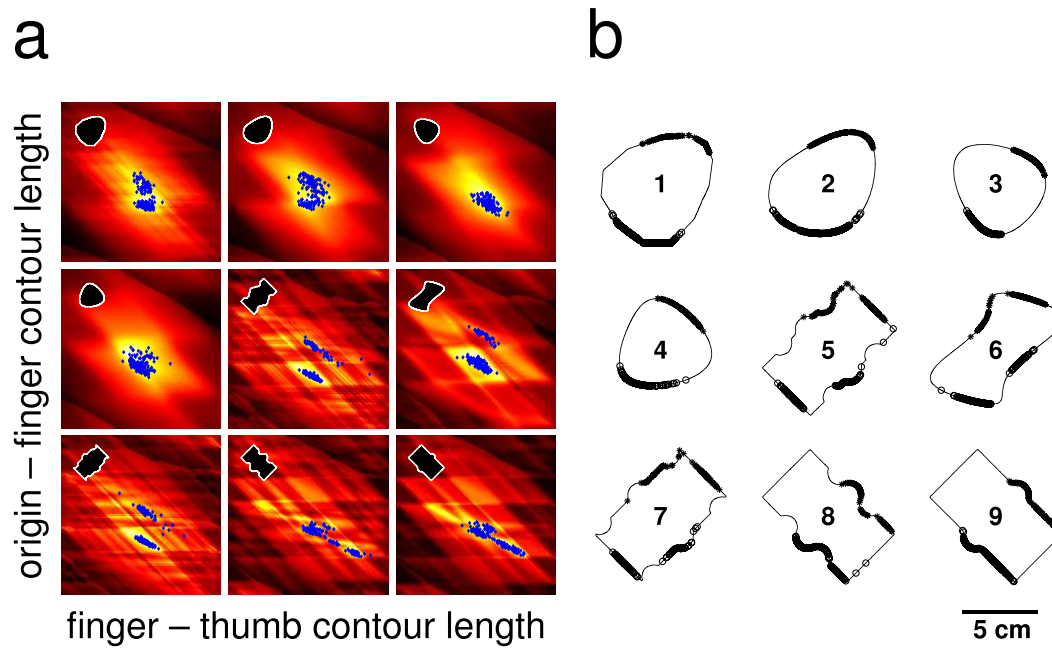
Figure 5. Complete penalty maps and contours of all objects used in Experiment 3. (a) Complete penalty maps with actual grasp points denoted as blue dots. The complete penalty maps are created by combining the individual penalty maps of each rule, for example, for object 5 in Figure 2. The high prediction quality of the CoPS model is reflected by the fact that the actual grasps (blue dots) are all in low penalty regions (white or yellow colored). For more details on the organization of the heat plots, see Figures 3 and 4. (b) Circles (stars) show actual contact points of the thumb (index finger) for all participants and grasps.

models we then compared model performance against the original CoPS model.

## Results

### Experiment 1

Figure 1a shows the chosen grasp angles from Experiment 1 along with the predictions of the conflicting rules. According to the model, the grasp chosen on average by participants is associated with the smallest penalty for the rules involved. Using this assumption we estimated the penalty function for this experiment (see data analysis). We obtained the penalty function for deviance from the NGA ($f_\alpha$) relative to the penalty function for deviance from perfect force closure ($f_\gamma$) with $f_\alpha(\alpha) = 1.77\ \alpha^{1.76}$ for the clockwise and $f_\alpha(\alpha) = .78\ \alpha^{1.9}$ for the counterclockwise direction of grasp axis rotation away from NGA. We also tested if participants adapted their grasp to the objects over the course of repeated presentation of the same object. We found that the chosen grasp angle did not depend on the number of object presentations, $F(2.356, 37.7) = 0.356$, $p = 0.737$, on Greenhouse-Geisser corrected $df$s.

### Experiment 2

Figure 1b shows the deviances from perfect force closure along with the predictions of the conflicting rules. From the data of Experiment 2 we could estimate the penalty function for the torque rule ($f_\tau$) relative to the function for deviance from perfect force closure ($f_\gamma$).

As has been mentioned already in the data analysis section, in Experiment 2 we observed that participants on average did not realize perfect force closure, even in the neutral object. One reason for this was a general undershoot in the average movement of participants. We observed a similar behavior to a lesser extent in Experiment 1 as well. To accommodate these findings, we included a penalty for longer movement distances ($\lambda$) as an additional rule $f_\lambda(\lambda)$ into the CoPS model. Only one parameter could be estimated for this distance rule, because it had not been subject to systematic variation (see Data analysis). It should also be noted that, depending on the orientation of the ellipsoid, barycenter distance and movement distance could covary. From our data we arrived at an estimate for the penalty functions $f_\tau(\tau) = 5.52 \times 10^3\ \tau^{1.82}$ and $f_\lambda(\lambda) = 4.87\lambda$. The complete penalty function for a given grasp according to the CoPS model thus reads

$$p = \gamma^2 + 1.77\alpha^{1.76} + 5.52\times10^3\tau^{1.82} + 4.87\lambda \qquad (11)$$

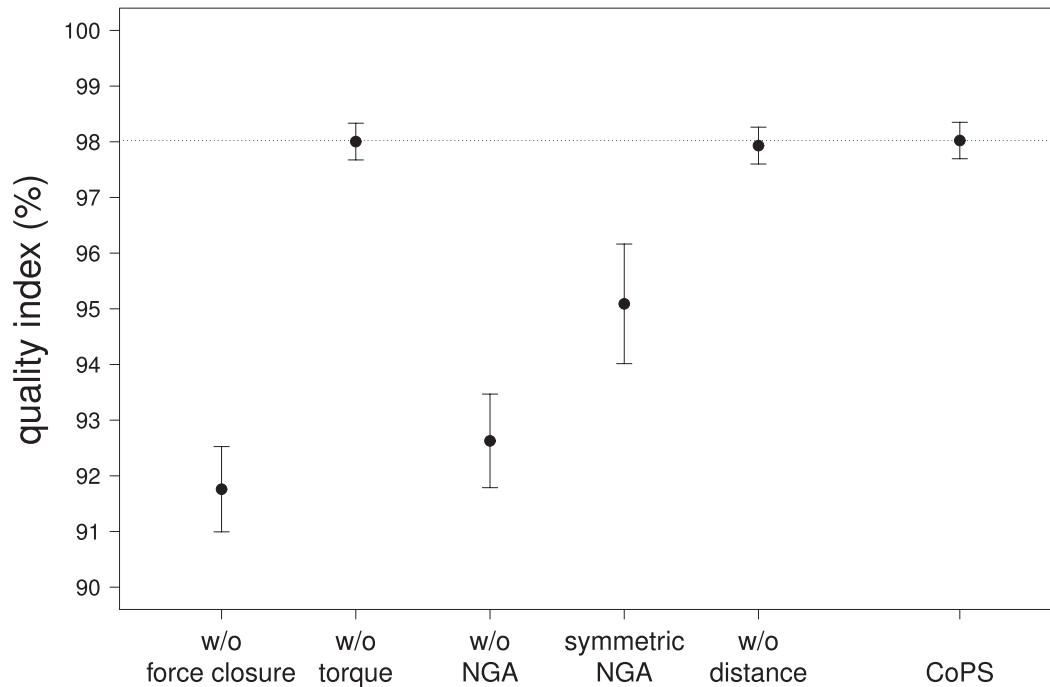for the clockwise direction of $\alpha$ and

Figure 6. Performance of five reduced models, each missing a part of the complete CoPS model. The *x*-axis annotation shows the difference from the complete CoPS model. Error bars show one standard error between subjects. The dotted line marks the performance of the CoPS model.

$$p = \gamma^2 + .78\alpha^{1.9} + 5.52 \times 10^3 \tau^{1.82} + 4.87\lambda \qquad (12)$$

for the counterclockwise direction of $\alpha$. Values for $\gamma$ and $\alpha$ are specified in rad, $\lambda$ in m, and $\tau$ in kg × m. Figure 2 shows a set of example grasps on a rectangular object in order to demonstrate equal penalties arising from different rule deviations.

A test for adaptation of the grasp over repeated object presentations was not significant, $F(4.508, 81.139) = 1.117$, $p = 0.356$, on Greenhouse-Geisser corrected *df*s.

## Experiment 3

For Experiment 3, penalty values for every possible grasp of the objects were calculated from the estimated parameters for the grasp rules. The corresponding values for the three main grasp rules are shown in Figure 3 for an exemplary object. Figure 4 shows all possible penalty map combinations for the same object, including the complete CoPS model according to Equations 11 and 12. Figure 5b shows the measured contact points on the complex objects of Experiment 3. Figure 5a shows the complete penalty maps with the measured grasps corresponding to these contact points (Note that because the objects were presented at the same orientation for every participant, the actual penalty map of a person depends on the individual NGA, which in Experiment 3 was determined by disc

trials as in Experiments 1 and 2. For the creation of the maps shown in Figures 3, 4, and 5a, however, the mean NGA of all participants from Experiment 3 was used for illustrative purposes.).

We measured the prediction quality of the CoPS model by means of a quality index ($q$), which indicates for each individual grasp how close it was to the prediction of the model. For each grasp, it is calculated which percentage of possible grasps would have received higher penalty values by the model. A value of $q = 100\%$ corresponds to a perfect prediction (participants always choose the grasp with the lowest penalty value; i.e., no other possible grasp has a lower penalty value). The mean value of the quality index across all objects and participants amounted to 98.02%, the lowest mean value for a single object being 96.97% and the highest being 99.11%.

## Simulation-based validation

In our test of the generality of the CoPS model we recalculated $q$ for every possible combination of object and map. The correct combination of object and map had a significantly higher quality index ($q = 98.02\%$) than the average of the control combinations ($q = 92.7\%$, $V = 171$, $p < 0.001$). Furthermore, there was no single control combination performing better than the correct combination of object and map.
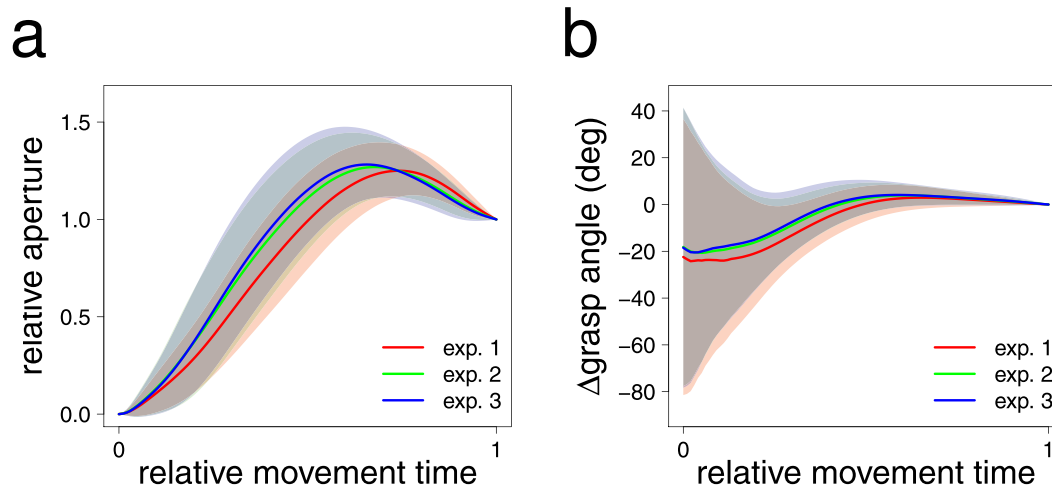
Figure 7. (a) Development of the relative aperture between index finger and thumb over the course of the movement. The relative aperture was calculated by subtracting the initial aperture at movement start and dividing by the final aperture at time of object contact. Values were time-normalized between movement start and end. Shaded areas indicate one standard deviation between participants. (b) Development of the grasp angle, i.e., the orientation of the digits when projected onto the horizontal surface. The figure shows the difference between the grasp angle during the movement and the final grasp angle at the end of the movement. Shaded areas indicate one standard deviation between participants.

## Importance of individual grasp rules

The mean quality indices of the comparison models and the complete CoPS model are shown in Figure 6. Excluding the force closure rule or the NGA rule resulted in large drops in performance down to 91.76% ($V = 171$, $p < 0.001$) and 92.63% ($V = 171$, $p < 0.001$), respectively. Excluding the torque rule had a relatively small effect on performance ($q = 98.00\%$ as compared to $q = 98.02\%$ in the complete CoPS model). Nevertheless, all participants improved on the majority of objects such that this difference was also significant in the nonparametric rank-based test we used ($V = 158$, $p < 0.001$). A slightly larger decrease in performance was found when excluding the distance rule ($q = 97.93\%$, $V = 167$, $p < 0.001$). Here, only one participant did not perform better on the majority of objects when including the rule. With both rules, there was a tendency that including the rule had a higher impact on performance with the more elongated objects (like e.g., objects eight and nine in Figure 5b), as compared to the rounded objects (e.g., objects one or two). Using a symmetrical NGA rule instead of two separate rules for clockwise and counterclockwise deviations from NGA

lead to a midsize drop in prediction quality ($q = 95.09$, $V = 162$, $p < 0.001$).

## Movement characteristics

In addition to the grasp-rule related analysis we also conducted an analysis of the kinematic properties of the measured grasp movements. In Figure 7 we show the relative aperture (Figure 7a) and the deviation from the final grasp angle during the movement (Figure 7b) as the digits are approaching the objects of the three experiments. In Table 1 we provide some of the main kinematic measures most commonly reported in precision grip grasp experiments.

## Discussion

We present a quantitative model of human grasp point selection. It embodies four rules whose penalty values are summed up to a final penalty for every possible grasp. The model successfully predicts human

| Measure | Experiment 1 | Experiment 2 | Experiment 3 |
|---|---|---|---|
| Reaction time, in ms | 352 (76) | 351 (80) | 332 (47) |
| Movement time, in ms | 861 (112) | 898 (131) | 895 (164) |
| Maximum grip aperture, in mm | 67 (5) | 65 (5) | 78 (9) |
| Time at maximum grip aperture, in ms | 632 (88) | 559 (88) | 556 (96) |

Table 1. Means (and standard deviations between participants) of kinematic characteristics of Experiments 1 through 3.

contact point choice using only object geometry and NGA as parameters.

Our model fills an important gap in current approaches to hand movement planning. Together with existing models for biologically inspired trajectory synthesis (Flash & Hogan, 1985; Uno, Kawato, & Suzuki, 1989; Harris & Wolpert, 1998; Smeets & Brenner, 1999) it allows for a complete synthesis of an artificial, yet human-like, grasp movement. Our results show that the human aspect is important. In fact, taking the NGA into account turned out to be as important as achieving force closure, which is by far the most important physical constraint to a grasping movement. Different platforms have been developed lately in the field of robotic hands (see Biagiotti, Lotti, Melchiorri, & Vassura, 2004; Ritter, Haschke, & Steil, 2009 for overviews), and algorithms for finding stable grasp points even on untrained objects are available (e.g., Chen & Burdick, 1993; Ponce et al., 1993; Borst, Fischer, & Hirzinger, 1999; Jia, 2002). These algorithms, however, don't necessarily mimic human behavior and can lead to grasps that are awkward or impossible to perform with a human hand. The advantage of the CoPS model is that it considers both human and physical stability constraints and thus finds the stable grasps naturally chosen by humans. In comparison to the NGA and force-closure rules, the torque and distance rules seemed to be of minor importance for the choice of appropriate grasp points. It should be kept in mind, however, that the corresponding analysis was conducted on the rather small set of objects of Experiment 3. These rules might well turn out to be of more importance when grasping objects with a more elongated shape, a different mass, or a more complex mass distribution as the ones used here.

An important application for grasp point selection is movement planning in brain machine interface (BMI) guided upper limb prostheses. Prosthesis rejection rate is still very high (over 20%; Biddiss & Chau, 2007). Reproducing the natural human goal choice will result in movements that more closely resemble real human action. This will likely make it easier for patients to incorporate an artificial limb into their body schema and raise acceptance of prostheses, both in patients and in their environment.

Using a model that mimics the human choice of grasp points may also allow for more efficiency in BMI guidance. Accurate guidance of BMIs on the basis of low level motor command signals can require a large amount of input data (Carmena et al., 2003; Lebedev et al., 2011). A way to increase efficiency is to decode action intentions and leave the detailed elaboration of the motor plan to an algorithm (Musallam, Corneil, Greger, Scherberger, & Andersen, 2004; Pesaran, Musallam, & Andersen, 2006). In monkeys, this "cognitive" approach can work successfully with very limited input data

(Musallam et al., 2004). Goal decoding as compared to position decoding can even be advantageous to performance when the signal is noisy (Marathe & Taylor, 2011; velocity decoding, however, also yielded a good performance). In such a "high level" BMI approach, the CoPS model plus a trajectory generator can improve efficiency by transforming the abstract action goal of grasping a particular object into a concrete, executable movement plan for the effector device.

With the CoPS model we present a deliberately simple and, therefore, robust method for predicting human grasp points. As the model omits higher cognitive aspects of movement planning, it does not capture, for example, task-dependent differences in grasping an object (see e.g., Rosenbaum et al., 1990; Crajé, Lukos, Ansuini, Gordon, & Santello, 2011; Sartori, Straulino, & Castiello, 2011). Another restriction is its limitation to two-digit precision grasp movements. Clearly there is a vast number of objects for which precision grasping can't be used. Also, not for all objects which can be grasped with a precision grip this will be the most preferred alternative (see e.g., Gilster, Hesse, & Deubel, 2012). On the other hand, a unified framework that is able to predict grip selection and hand, palm, or digit placement is missing at the moment. Therefore, solving the problem for subclasses of grips can be considered a good first point to start.

## Conclusion

Human contact point selection in precision grip grasping can successfully be predicted by considering four basic grasp rules: Force closure, torque, natural grasp angle, and movement distance. From these four rules, two are the most important for human graspers: getting a good force closure grip and realizing ones own natural grasp angle. By using a simple model incorporating these grasp rules, it may be possible to more efficiently guide human hand and arm prostheses.

*Keywords: grasping, contact point selection, motor control, modeling, hand prostheses*

## Acknowledgments

Commercial relationships: none.
Corresponding author: Urs Kleinholdermann.
Email: urs@kleinholdermann.de.
Address: Department of Experimental Psychology,
University of Giessen, Giessen, Germany.

# References

Biagiotti, L., Lotti, F., Melchiorri, C., & Vassura, G. (2004). *How far is the human hand? A review on anthropomorphic robotic end-effectors* (Internal Report). Bologna, Italy: DEIS–University of Bologna.

Biddiss, E. A., & Chau, T. T. (2007). Upper limb prosthesis use and abandonment: A survey of the last 25 years. *Prosthetics and Orthotics International, 31*(3), 236–257.

Blake, A. (1992). Computational modelling of hand–eye coordination. *Philosophical Transactions of the Royal Society of London, Series B–Biological Sciences, 337*(1281), 351–360.

Blake, A. (1995). A symmetry theory of planar grasp. *International Journal of Robotics Research, 14*(5), 425–444.

Borst, C., Fischer, M., & Hirzinger, G. (1999). A fast and robust grasp planner for arbitrary 3D objects. *Proceedings of the IEEE International Conference on Robotics and Automation, 3*, 1890–1896.

Carmena, J. M., Lebedev, M. A., Crist, R. E., O'Doherty, J. E., Santucci, D. M., Dimitrov, D. F., et al. (2003). Learning to control a brain–machine interface for reaching and grasping by primates. *PLoS Biology, 1*(2), E42.

Cattaneo, L., Voss, M., Brochier, T., Prabhu, G., Wolpert, D. M., & Lemon, R. N. (2005). A cortico-cortical mechanism mediating object driven grasp in humans. *Proceedings of the National Academy of Sciences, USA, 102*(3), 898–903.

Chen, I., & Burdick, J. (1993). Finding antipodal point grasps on irregularly shaped objects. *IEEE Transactions on Robotics and Automation, 9*(4), 507–512.

Crajé, C., Lukos, J. R., Ansuini, C., Gordon, A. M., & Santello, M. (2011). The effects of task and content on digit placement on a bottle. *Experimental Brain Research, 212*(1), 119–124.

Cuijpers, R. H., Smeets, J. B. J., & Brenner, E. (2004). On the relation between object shape and grasping kinematics. *Journal of Neurophysiology, 91*(6), 2598–2606.

Flash, T., & Hogan, N. (1985). The coordination of arm movements: An experimentally confirmed mathematical model. *Journal of Neuroscience, 5*(7), 1688–1703.

Ganel, T., & Goodale, M. A. (2003). Visual control of action but not perception requires analytical processing of object shape. *Nature, 426*(6967), 664–667.

Gilster, R., Hesse, C., & Deubel, H. (2012). Contact points during multidigit grasping of geometric objects. *Experimental Brain Research, 217*(1), 137–151.

Goodale, M. A., Meenan, J. P., Bülthoff, H. H., Nicolle, D. A., Murphy, K. J., & Racicot, C. (1994). Separate neural pathways for the visual analysis of object shape in perception and prehension. *Current Biology, 4*(7), 604–610.

Goodale, M. A., Milner, A. D., Jakobson, L. S., & Carey, D. P. (1991). A neurological dissociation between perceiving objects and grasping them. *Nature, 349*(6305), 154–156.

Goodale, M. A., Pelisson, D., & Prablanc, C. (1986). Large adjustments in visually guided reaching do not depend on vision of the hand or perception of target displacement. *Nature, 320*(6064), 748–750.

Harris, C. M., & Wolpert, D. M. (1998). Signal-dependent noise determines motor planning. *Nature, 394*(6695), 780–784.

Iberall, T., Bingham, G., & Arbib, M. A. (1986). Opposition space as a structuring concept for the analysis of skilled hand movements. *Experimental Brain Research Series, 15*, 158–173.

Jeannerod, M. (1984). The timing of natural prehension movements. *Journal of Motor Behavior, 16*(3), 235–254.

Jeannerod, M. (1986). The formation of finger grip during prehension: A cortically mediated visuo-motor pattern. *Behavioral Brain Research, 19*(2), 99–116.

Jia, Y.-B. (2002). Curvature-based computation of antipodal grasps. *Proceedings of the IEEE International Conference on Robotics and Automation, 2*, 1571–1577.

Lebedev, M. A., Tate, A. J., Hanson, T. L., Li, Z., O'Doherty, J. E., Winans, J. A., et al. (2011). Future developments in brain–machine interface research. *Clinics, 66*(S1), 25–32.

Lederman, S. J., & Wing, A. M. (2003). Perceptual judgment, grasp point selection and object symmetry. *Experimental Brain Research, 152*(2), 156–165.

Lukos, J., Ansuini, C., & Santello, M. (2007). Choice of contact points during multidigit grasping: Effect of

predictability of object center of mass location. *Journal of Neuroscience, 27*(14), 3894–3903.

Mangialardi, L., Mantriota, G., & Trentadue, A. (1996). A three-dimensional criterion for the determination of optimal grip points. *Robotics & Computer-Integrated Manufacturing, 12*(2), 157–167.

Marathe, A. R., & Taylor, D. M. (2011). Decoding position, velocity, or goal: Does it matter for brain–machine interfaces? *Journal of Neural Engineering, 8*(2), 025016.

Milgram, P. (1987). A spectacle-mounted liquid-crystal tachistoscope. *Behavior Research Methods, Instruments, & Computers, 19*(5), 449–456.

Musallam, S., Corneil, B. D., Greger, B., Scherberger, H., & Andersen, R. A. (2004). Cognitive control signals for neural prosthetics. *Science, 305*(5681), 258–262.

Nguyen, V.-D. (1986). Constructing stable force-closure grasps. *Proceedings of the 1986 ACM Fall Joint Computer Conference.* (pp. 129 137). Los Alamitos, CA, USA: IEEE Computer Society Press.

Pesaran, B., Musallam, S., & Andersen, R. A. (2006). Cognitive neural prosthetics. *Current Biology, 16*(3), R77–R80.

Ponce, J., Stam, D., & Faverjon, B. (1993). On computing force-closure grasps of curved two-dimensional objects. *International Journal of Robotics Research, 12*(3), 263–273.

R Development Core Team. (2011). *R: A language and environment for statistical computing.* Vienna, Austria: R Foundation for Statistical Computing.

Ritter, H., Haschke, R., & Steil, J. J. (2009). Trying to grasp a sketch of a brain for grasping. In B. Sendhoff, K. Doya, E. Körner, O. Sporns, H. Ritter (Eds.). *Creating brain-like intelligence* (pp. 84–102). Heidelberg, Germany: Springer-Verlag Berlin.

Rosenbaum, D. A., Marchak, F., Barnes, H. J., Vaughan, J., Slotta, J. D., & Jorgensen, M. J. (1990). Constraints for action selection: Overhand versus underhand grips. In M. Jeannerod (Ed.), *Attention and performance XIII: Motor Representation and Control* (pp. 321–345). Hillsdale, NJ: Lawrence Erlbaum Associates.

Sanz, P. J., Iñesta, J. M., & del Pobil, A. P. (1999). Planar grasping characterization based on curvature–symmetry fusion. *Applied Intelligence, 10*(2), 25–36.

Sartori, L., Straulino, E., & Castiello, U. (2011). How objects are grasped: The interplay between affordances and end-goals. *PLoS One, 6*(9), e25203.

Smeets, J. B. J., & Brenner, E. (1999). A new view on grasping. *Motor Control, 3*(3), 237–271.

Uno, Y., Kawato, M., & Suzuki, R. (1989). Formation and control of optimal trajectory in human multi-joint arm movement: Minimum torque-change model. *Biological Cybernetics, 61*(2), 89–101.

Whitney, D., Westwood, D. A., & Goodale, M. A. (2003). The influence of visual motion on fast reaching movements to a stationary object. *Nature, 423*(6942), 869–873.